

## Modeling a large solar proton event in the southern polar atmosphere

Mark A. Clilverd,<sup>1</sup> Craig J. Rodger,<sup>2</sup> Thomas Ulich,<sup>3</sup> Annika Seppälä,<sup>4</sup> Esa Turunen,<sup>3</sup> Aurelein Botman,<sup>1</sup> and Neil R. Thomson<sup>2</sup>

Received 26 November 2004; revised 14 April 2005; accepted 19 April 2005; published 17 September 2005.

[1] We have modeled the effects of the Sodankylä Ion Chemistry model (SIC) electron density profiles on VLF propagation across the southern polar region during the first few days of the 4–10 November 2001 solar proton event (SPE). The results show that the SIC model is accurately reproducing the changes in ionization during the SPE. These results were obtained by approximating the SIC electron density profiles to the Wait  $\beta$  and  $h'$  profiles where the densities were below  $1000 \text{ el cm}^{-3}$ , a limitation that means during SPEs the technique is typically sensitive in the altitude range 50–60 km. The calculated values of  $\beta$  and  $h'$  were applied to the part of the propagation path poleward of the  $L = 4$  boundary for the Hawaii (NPM)–Halley great circle path. Comparing the change in amplitude of NPM at Halley during the SPE with the GOES satellite proton flux measurements, we observe a good correlation and thus conclude that the variability observed in the VLF data is primarily caused by  $>50 \text{ MeV}$  proton fluxes. This suggests that the SPE produced ionization dominates all other precipitation sources at these altitudes during 4 and 5 November 2001. Consequently, these results suggest that the assumption made during the SIC modeling runs of 4–5 November 2001 of only having proton precipitation and no significant energetic electron precipitation was reasonable. Our work strongly suggests that VLF subionospheric propagation is a reliable tool for the study of SPEs and that it is particularly effective when used in conjunction with an atmospheric model such as SIC.

**Citation:** Clilverd, M. A., C. J. Rodger, T. Ulich, A. Seppälä, E. Turunen, A. Botman, and N. R. Thomson (2005), Modeling a large solar proton event in the southern polar atmosphere, *J. Geophys. Res.*, 110, A09307, doi:10.1029/2004JA010922.

### 1. Introduction

[2] During solar proton events (SPE), high-energy precipitation, penetrating deep into the Earth's atmosphere, affects the whole of the polar regions down to about  $60^\circ$  geomagnetic latitude,  $L = 4$  [Reagan and Watt, 1976]. Below  $\sim 100 \text{ km}$  altitude the energy input during a SPE is known to increase ionization and significantly affect the neutral chemistry, such as causing large depletions of ozone at high latitudes [Solomon *et al.*, 1983; Reid *et al.*, 1991; Jackman *et al.*, 1993]. SPEs occur relatively infrequently and show high variability in their intensity and duration [Shea and Smart, 1990]. Satellite data show that the protons involved have an energy range spanning 1 to 500 MeV. Events tend to occur more frequently during solar maximum conditions, such as those that existed during 2000–2001. For large events the duration is typically several days, with

rise times of  $\sim 1$  hour, and a slow decay to normal flux values thereafter [Reeves *et al.*, 1992].

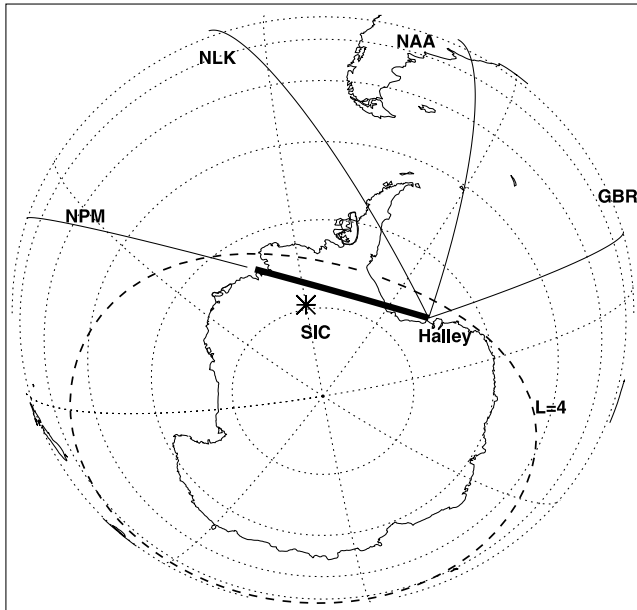
[3] Very low frequency (VLF) radio signals, or long-wave radio signals, are known to be severely affected during SPEs. Early work by Potemra *et al.* [1967] analyzed phase anomalies in VLF transmissions during a SPE in February 1965, connecting the observed changes to solar proton fluxes measured by satellite. These signals can be thought of as propagating in a waveguide formed by the surface of the Earth and the lower boundary of the reflective ionosphere at around 50–100 km altitude (see Barr *et al.* [2000] for a substantive review). During a SPE the effective height of the ionosphere is changed through enhanced ionization at lower altitudes, leading to a modification of the wave propagation conditions, thus changing signal amplitude and phase as measured at a fixed receiver position [Potemra *et al.*, 1967; Cummer *et al.*, 1997]. The Naval Ocean Systems Center (NOSC) provide a code (LWPC, Long Wave Propagation Code) to model VLF signal propagation from any point on Earth to any other point. Given electron density profile parameters for the upper boundary conditions, LWPC calculates the expected amplitude and phase at the reception point [Ferguson and Snyder, 1990]. Thus it can be used to investigate the modification of the ionosphere during SPEs, characterizing

<sup>1</sup>British Antarctic Survey (NERC), Cambridge, UK.

<sup>2</sup>Physics Department, University of Otago, Dunedin, New Zealand.

<sup>3</sup>Sodankylä Geophysical Observatory, University of Oulu, Sodankylä, Finland.

<sup>4</sup>Finnish Meteorological Institute, Helsinki, Finland.



the electron density profile produced by the precipitating particle fluxes. When a VLF propagation path crosses low conductivity ground such as the Antarctic or Greenland ice caps, the effect of the SPE is enhanced, allowing sensitive modeling of the SPE effect to be made [Westerlund *et al.*, 1969]. One such transmitter to receiver path that can be used for this type of study is Hawaii (NPM, 21.4 kHz) to Halley, Antarctica, (75.5°S, 26°W). Approximately 2000 km of this great circle path passes through the Southern Hemisphere polar region and should be strongly influenced by SPE conditions.

[4] The Sodankylä Ion Chemistry model (SIC) [see Verronen *et al.*, 2002] models the major chemical reactions and interactions known to occur in the lower ionosphere. Given input conditions such as precipitating particle fluxes, the model produces (among other things) positive and negative ion density profiles from which electron density profiles at altitudes 50–150 km are extracted. These profiles can be passed to LWPC to model the signal levels for an actual event. Thus it is possible to compare the performance of the SIC and LWPC models against real (measured) solar proton event data. Previously, the SIC model ionization calculations has been compared with 2 hours of averaged EISCAT electron density data [Verronen *et al.*, 2002]. Here we use continuous ground-based VLF propagation signals recorded at Halley to provide comparison for the SIC model during the onset and main phase of a solar proton event, 36 hours in all.

[5] In this study we make a detailed comparison of model results and in situ observations of the impact in the southern polar atmosphere of the intense solar proton event that started on 4 November 2001 through changes produced

by the energetic precipitation into the atmosphere (<100 km). We study the SPE during 4 and 5 November 2001, when large fluxes of high-energy protons were observed at geostationary orbits. We show that a complex model of the atmosphere (SIC) can accurately represent the ionization changes that occurred at high southern latitudes.

## 2. Experimental Setup

[6] At Halley, Antarctica, (75°36'S, 26°19'W,  $L = 4.5$ ) a VLF receiver was used to monitor the phase and amplitude of several high-powered transmitters located in the Northern Hemisphere [Dowden *et al.*, 1994; Clilverd *et al.*, 2001]. Although Halley lies near the outer edge of the “average” area affected by SPE's ( $L = 4$  requires a proton energy of over 500 MeV to reach ground level), some of the great circle paths (GCP) taken by the signals to reach the receiver at Halley go through the polar region and are expected to be significantly influenced during SPEs, as shown in Figure 1. The bold part of the NPM-Halley great circle path (GCP) line shows where the VLF signal from Hawaii (NPM) goes through the polar region. The signals from other transmitter sites such as Rugby, UK (GBR), Cutler, Maine (NAA), and Jim Creek, Washington (NLK), do not cross the polar region. Thus Halley is in a good position to observe both strongly affected signals and nonaffected ones during SPEs. Because of difficulties encountered in unambiguously unwrapping the phase data from NPM during this study, we confine ourselves to descriptions of the SPE effects on the amplitude data.

[7] The Sodankylä Ion Chemistry (SIC) model was run for the SPE conditions that occurred on 4 and 5 November 2001. Model runs were produced at 79.5°S, 270°E ( $L = 5.9$ ). This position is marked with an asterisk in Figure 1. The GCP of the NPM transmitter received at Halley passes close to the SIC analysis location, deep within the polar region, and the induced signal changes on NPM during the SPE can thus be compared with the SIC model results. We outline the model details and setup for SPE analysis in the sections below.

## 3. Sodankylä Ion Chemistry (SIC) Model

[8] The Sodankylä Ion Chemistry (SIC) model is a one-dimensional chemical model designed for ionospheric D-region studies, solving the concentrations of 63 ions, including 27 negative ions, and 11 neutral species between 50–150 km altitude. Several hundred reactions are implemented, plus external forcing due to solar radiation (1–422.5 nm), electron and proton precipitation, and galactic cosmic radiation. Initial descriptions of the model are provided by Turunen *et al.* [1996], with neutral species modifications described by Verronen *et al.* [2002]. Solar flux is calculated with the SOLAR2000 model (version 2.21) [Tobiska *et al.*, 2000]. The scattered component of Lyman- $\alpha$  solar flux is included using the empirical approximation given by Thomas and Bowman [1986]. Atomic nitrogen production through ion reactions is included in the basic ion reactions. Additional contributions from auroral secondary electrons are calculated using a parameterization which assumes the production rate of nitrogen atoms to be equal to 0.8 $Q$  [Rusch *et al.*,

1981], where  $Q$  is the total ionization rate due to protons, electrons, and galactic cosmic radiation. The latest extension of SIC is the vertical transport code [Chabrilat *et al.*, 2002] which takes into account molecular [Banks and Kockarts, 1973] and eddy diffusion [Ebel, 1980]. The background neutral atmosphere is calculated using the MSISE-90 model [Hedin, 1991]. Transport and energy are advanced in intervals of 5 or 15 min, and within each interval exponentially increasing time steps are used because of the wide range of chemical time constant of modeled species.

[9] Here we use the SIC model results generated at 79.5°S, 270°E. We investigate changes in the electron density profile in the D-region caused by solar proton precipitation. Detailed SIC calculations at this location have been done as part of a complementary study using the ODIN satellite. They show large reductions of ozone at 60 km during SPEs, along with significant enhancements of odd nitrogen, that are being compared with similar measurements made on board Odin [Murtagh *et al.*, 2002; A. Seppälä, manuscript in preparation, 2005].

[10] In the solar proton event the proton spectra at the top of the atmosphere is assumed to be the same as those measured by GOES-08 at geosynchronous altitude. This assumption is valid for high magnetic latitudes. The angular distribution of the protons is assumed to be isotropic over the upper atmosphere, which is valid close to the Earth [Hargreaves, 1992]. Although the SIC modeling was undertaken for the SPE conditions that occurred during 4 and 5 November 2001, with a proton spectra it is possible that there was also significant high-energy electron precipitation at the same time [Shirochkov *et al.*, 2004], and that this would influence the amounts of ionization occurring during the SPE. As a result the model ozone depletion levels could be unrealistic, but the satellite data during the event was too sparse to check this. The comparison with VLF propagation data from Halley will allow this potential uncertainty in the modeling to be assessed.

#### 4. The 4–10 November 2001 Solar Proton Event Overview

[11] For the solar proton event of 4–10 November 2001, the peak flux was  $31,700 \text{ cm}^{-2} \text{ sr}^{-1} \text{ s}^{-1}$  for proton energies  $>10 \text{ MeV}$ . The event started with a sudden increase in particle flux at 1600 UT on 4 November 2001, reaching high levels by 1800 UT, and remaining high until the end of 5 November, and then taking several more days to return back to prestorm levels. Levels of geomagnetic activity showed only a slow increase from the start of the SPE, with disturbed  $K_p = 5$  conditions only occurring late on 5 November, before peaking at  $K_p = 9$ —early on 6 November. We analyze this event in part because of the significance of the large fluxes involved, and in part because of the analysis already undertaken at 79.5°S, 270°E by SIC modelers (A. Seppälä, manuscript in preparation, 2005).

#### 5. Quiet Day Conditions

[12] The amplitude QDC is shown in Figure 2 with an indication of the variability given by a 3-sigma standard deviation line either side of the average. Eight days were

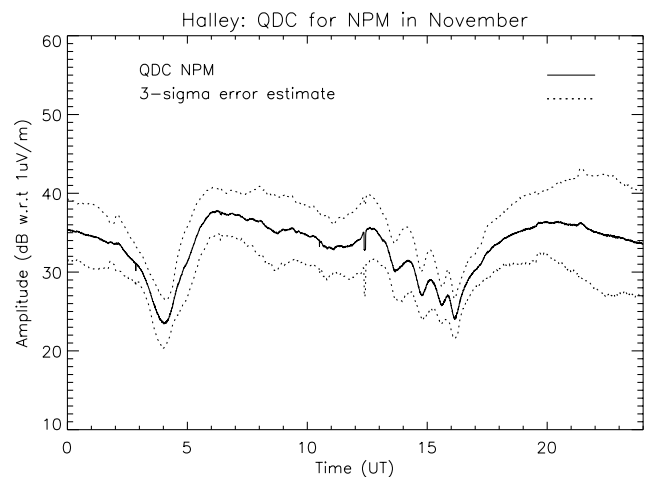


**Figure 2.** “Quiet-day” curve example: amplitude of signal from NPM in November 2001, with 3-sigma errors.

used to provide the average behavior line and were chosen when 3-hourly  $K_p$  was  $\leq 4$  throughout the day. In November most of the GCP is in daylight between the hours of 1700 and 0400 UT. This can be seen in the plot as the relatively smooth curve, as the ionospheric electron density profile is dominated at this time by the solar zenith angle. Modal minima are seen when the daylight terminator (the line between day and night) sweeps across the signal path and causes very large but repeatable changes in the modal makeup of the standing wave [see Clilverd *et al.*, 1999; Clilverd *et al.*, 2001]. Sunrise conditions on the GCP occur during 1400–1700 UT, while sunset conditions occur at 0500 UT. Small step-like features occur occasionally in the QDC (e.g.,  $\sim 1200 \text{ UT}$ ) which are as a result of either transient transmit power changes or short-lived features like solar flares. Averaging over 8 days in the month has essentially removed these features. Although some of traces of solar flare effects do remain (as seen in Figure 2), they do not significantly influence the results of this study.

[13] From 0000 UT on 4 November 2001 to 2300 UT on 5 November 2001 the SIC model was run to investigate atmospheric changes in the southern polar region caused by the SPE that occurred during that period. The model was used to generate hourly electron density profile curves as a function of altitude. In this study we analyze the SIC electron density profile information during the start and main phase of the SPE (4 November, 1200 UT to 5 November, 2300 UT). In order to be able to apply the results to LWPC the SIC curves were approximated using equation (1) (below), characterized by two parameters  $\beta$  and  $h'$ , and as a result they can be easily applied to the propagation code LWPC

$$N(z) = (1.43 \times 10^7) e^{(\beta-0.15)z-\beta h'} \quad (1)$$

This is a standard formulation [see, e.g., Wait and Spies, 1964] and describes the electron density of the lower ionosphere through  $h'$  (km), which represents the modified effective “reflection” height of the ionosphere, and  $\beta$  ( $\text{km}^{-1}$ ), for the “steepness” of the profile. The determina-

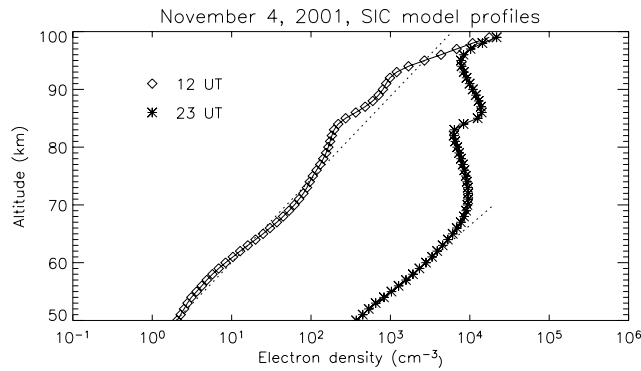


**Figure 3.** Electron density profiles. The two curves represent SIC model predicted values for the 4 November 2001 (1200 and 2300 UT), and the two straight lines represent the exponential profile approximation to the SIC model results.

tion of the parameters was done by least-squares fitting equation (1) to the SIC profiles below  $1000 \text{ el cm}^{-3}$ , as at the electron densities above this height have little effect on subionospheric propagation.

[14] The SIC model electron density profiles during 4 November 2001 (at 1200 and 2300 UT) can be seen in Figure 3; the curves are the SIC predicted profiles, and the straight lines are the  $\beta$  and  $h'$  approximation to those curves. During the hours that SIC was run before the start of the SPE (1200–1600 UT) the fitted  $\beta$  and  $h'$  values were very consistently  $\beta = 0.30 \text{ km}^{-1}$  and  $h' = 77.6 \text{ km}$ . This value of  $\beta$  is very similar to low and midlatitude values of  $\beta$  found

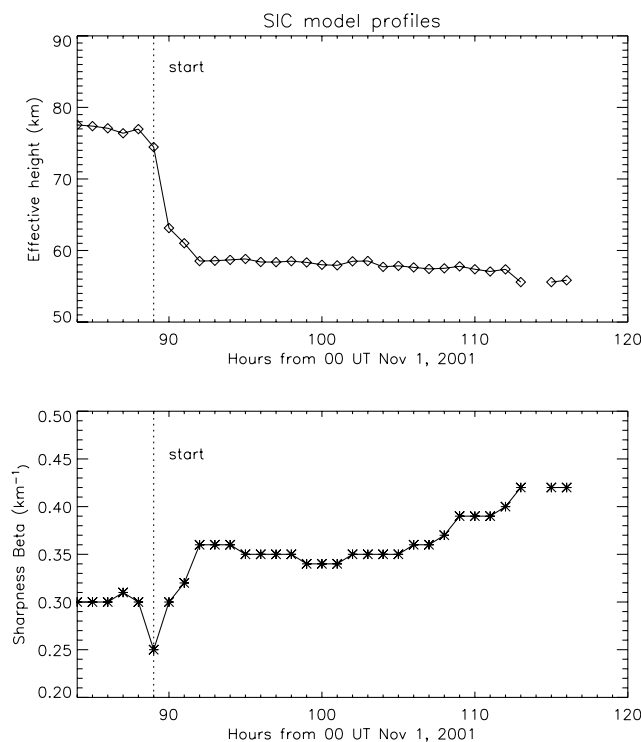


**Figure 4.** The evolution of the estimated sharpness ( $\beta$ ) and effective height ( $h'$ ) values during 4 and 5 November 2001 SPE.

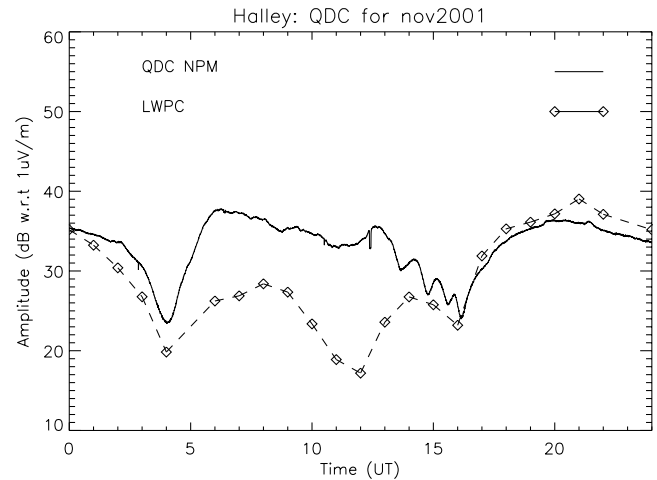


**Figure 5.** Plot of measured QDC for signal from NPM (solid line), with the LWPC-predicted QDC (diamond/dashed line).

from VLF propagation measurements at similar (high) solar zenith angles. The value of  $h'$  is  $\sim 3 \text{ km}$  higher than the corresponding value from lower latitudes. After the onset of the energetic particle precipitation caused by the SPE the  $\beta$  and  $h'$  rapidly adjust to  $\beta = \sim 0.40 \text{ km}^{-1}$  and  $h' = \sim 60 \text{ km}$ . This is consistent with the generation of ionization well below the normal altitudes of the ionosphere, and with a steeper gradient of change with altitude at the lower edge where VLF waves are likely to be incident. The evolution of  $\beta$  and  $h'$  values during the whole event can be seen in Figure 4. This shows that both the lowering of the effective ionosphere height ( $h'$ ), and the rise in the electron profile steepness ( $\beta$ ) is maintained throughout the period of high particle fluxes. Beyond hour 116 the fitting routine used on the SIC profiles was unable to cope as the  $1000 \text{ el cm}^{-3}$  limit occurred below the SIC lowest altitude (50 km). No values are plotted, or further simulations made, after this time.

[15] The LWPC model was run to produce an equivalent model QDC for November, with the code's default electron density profiles for the conditions along the GCP from NPM to the edge of the polar region, i.e., at  $75^\circ\text{s}$ ,  $105^\circ\text{W}$ , and then using the SIC quiet-time  $\beta$  and  $h'$  from there to Halley, i.e., the last 2400 km of the path. This approach is reasonable as the LWPC southern polar ionospheric parameters change little over these distances, making the offset in location of the SIC modeling and the NPM GCP insignificant. This technique produces a model diurnal variation, which can be compared with the observed QDC for November, see Figure 5. The values on the y-axis are in dB w.r.t  $1 \mu\text{V m}^{-1}$ . LWPC produces absolute values based on actual transmitter output powers (in the case of NPM, 500 kW). The NPM QDC is also in calibrated units, and thus we see that there is very close agreement between the modeling technique and the actual recorded data. The fit is particularly close during daylight conditions on the GCP (1700–0300 UT), but during the nighttime portion of the diurnal curve, i.e., 0400–1600 UT, the absolute values and variation with time are less well represented by LWPC, with discrepancies of typically  $-10 \text{ dB}$ . This suggests that the

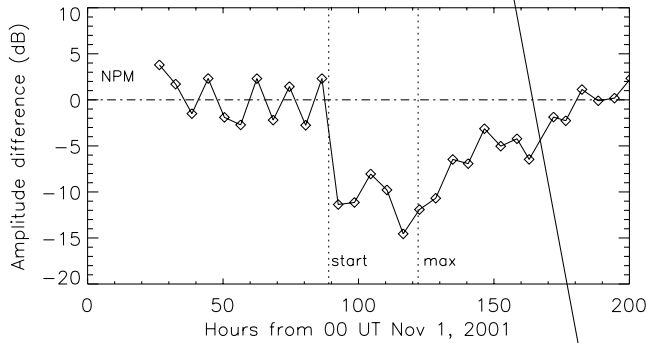


**Figure 6.** The SPE effects on the signals from NPM after the QDC has been subtracted. Hourly data points have been smoothed with a 6 hour running mean to reduce scatter.

model is accurately reproducing the modal makeup of the NPM signal, even across the polar section of the path.

## 6. SPE Effects

[16] Once the QDCs have been determined for each of the transmitter signals of interest, they can be subtracted from the data during the SPE period of interest. Figure 6 shows the deviations of the NPM signal from its QDC during the first 200 hours of November 2001, i.e., from 1 to 8 November. The hourly data used have been smoothed in order to clarify the plot (see caption for details). The times of the start and maximum of the SPE are indicated by vertical dotted lines. The plot clearly shows the significant absorption of the NPM signal, coincident with the onset of the SPE, and reaching a maximum effect of  $\sim -15$  dB close to the maximum of the SPE. A gradual recovery lasting about 70 hours after the maximum can also be seen.

[17] Although the NPM signal experienced 15 dB of absorption during the SPE, it is important to note here that the signal was still above the local noise floor during that period. Analysis revealed that at several times during the event the signal amplitude level went below the noise level expected for that time of day but without loss of phase data which usually flags the descent into noise levels. It was found that at these times, the noise level was lower than at equivalent times on a quiet day. The difference was typically 3 or 4 dB and caused by attenuation of lightning noise from some of the distant lightning sources like Africa or India. Thus we can be confident that the measured absorption levels are well known and not restricted by signal-to-noise limits.

[18] To model the effect of the SPE on NPM the  $\beta$  and  $h'$  values obtained from the SIC model were applied to the LWPC model to represent a modified electron density profile in the polar region. The SIC profiles were applied to the same length polar part of the path for every calculation. This technique does not therefore take into account any variations in the geomagnetic latitude of the cutoff energy of the solar protons with local time or  $K_p$ , although the effects are expected to be relatively small on the long path involved here. This was done for each hour of the SIC model runs (36 hours, starting from 1200 UT, 4 November 2001), with

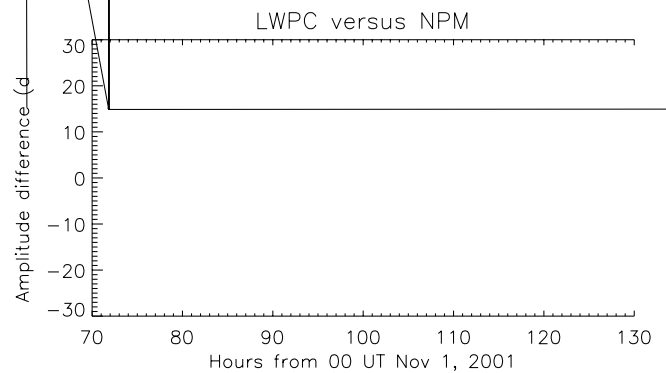
the previously described LWPC QDC for NPM subtracted. Figure 7 shows an hourly intercomparison between the data and the LWPC results. The start and maximum times of the SPE are shown by vertical dotted lines as before. The solid line represents the recorded data, while the diamonds represent the LWPC model results. Close agreement can be seen between the two data sets. The model slightly overestimates the effect of the solar proton event for the first few hours but thereafter convincingly captures the variability observed during the hours 95–115. Periods when the data show rapid fluctuations such as just before the SPE start time are caused by differences in the sunrise/sunset model minima levels compared with the average QDC. Changes in the depth of modal minima can often be significant even from day-to-day. The plot shows that using the technique of imposing the SIC electron density profiles on the propagation conditions in the polar section of the propagation path can accurately model the changes in the recorded NPM signal, which implies there were no significant effects from electron precipitation.

### 6.1. Relationship With Particle Fluxes

[19] Early work on the effects of SPEs on radio propagation showed that a range of responses could be anticipated from the received amplitude of high-latitude signals, i.e., either increases or decreases in amplitude. In Figure 8 we show the SPE effect on NPM, and the  $>50$  MeV GOES fluxes during the same time period. The fluxes have been scaled according to the following formula:

$$\Delta NPM(dB) = -1.3 \times \log_e(f_{50}) - 3.5, \quad (2)$$

where  $f_{50}$  is the  $>50$  MeV proton flux in  $\text{cm}^{-2} \text{sr}^{-1} \text{s}^{-1}$ . A relationship of this form was suggested by *Westerlund et al.* [1969] for phase changes on signals propagating over Greenland. This is reasonable in that the high-energy part of the proton spectrum should be influencing the lowest part of the ionosphere and thus interacting with VLF propagation conditions. The higher-energy part of the proton spectrum will penetrate to lower altitudes and form



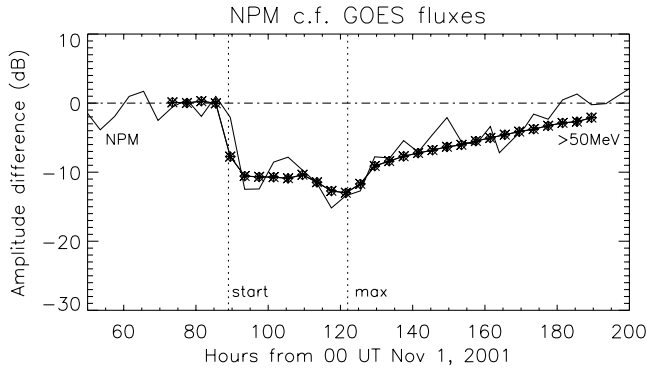


**Figure 8.** A comparison of the observed variation of the amplitude of NPM during the SPE with that calculated from the  $>50$  MeV proton fluxes from GOES-08 using equation (2).

the lower D-region boundary during the solar proton event [see *Rishbeth and Garriott, 1969, Figure 26*]. The grazing incidence VLF waves only interact with the lower boundary of the ionosphere and thus are insensitive to lower-energy protons producing higher-altitude ionization when higher-energy fluxes are present. We also tested (not shown) the relationship for  $>1$  MeV,  $>10$  MeV, and  $>100$  MeV proton fluxes. Here  $>1$  MeV and  $>10$  MeV fluxes continued well after the NPM absorption effect had stopped, while the  $>100$  MeV fluxes ended just prior to it. The  $>50$  MeV fluxes correlation coefficient was high at 0.82 and also showed high significance. Toward the end of the solar proton event, when the high-energy protons have returned to quiet time levels, the continuing lower energy fluxes are the most important D-region ionization source and thus form the lower D-region boundary, but this effect is too small to be observable on the NPM-Halley GCP, as Figure 8 shows. Clearly, despite previous observations of a variety of amplitude behavior during SPEs, some paths allow a good comparison between the observed behavior and proton fluxes.

[20] As we can not apply equation (2) to other propagation paths and conditions, it would be better to generalize the relationship to proton fluxes using the ionospheric parameters  $\beta$  and  $h'$ . Figure 9 shows the result of plotting the parameters against  $>50$  MeV proton fluxes. Clearly,  $h'$  shows a good correlation with proton fluxes. As the value of  $\beta$  was essentially unchanged during the first few hours of the SPE, it appears that the proton fluxes must reach a threshold level before any significant influence occurs on the sharpness of the lower D-region. This threshold is depicted in Figure 9 by the vertical dotted line. The seemingly complex behavior of  $\beta$  requires further investigation during other events. Together the ionospheric parameters show that as the proton flux increases the lower edge of the D-region ionosphere decreases in altitude and then becomes sharper (just as during a solar flare). The relationship between the flux and  $h'$  can be represented by

$$h' = 71 - 2.5 \times \log_e(f_{50}) \text{ km.} \quad (3)$$

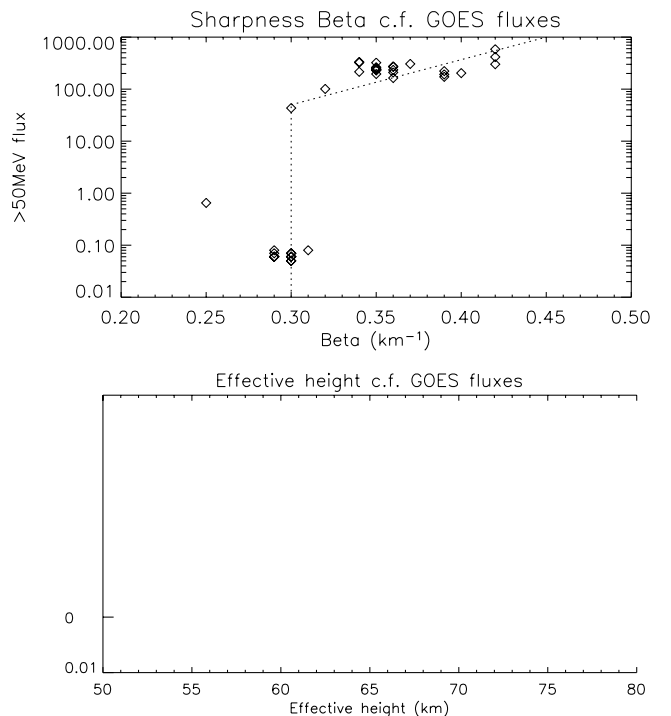
In the  $h'$  equation the offset value is close to normal daytime D-region conditions. It is unclear if this will hold for polar

night conditions. This relationship will be compared against the results obtained during other SPEs in a future paper.

## 7. Discussion and Summary

[21] We have used the Wait ionospheric parameterization to model the effects of the SIC model electron density profiles on VLF propagation across the southern polar region. The results show that the SIC model is accurately reproducing the changes in ionization during the SPE of 4–5 November 2001 (see Figure 7). These results were obtained by approximating the SIC electron density profiles to  $\beta$  and  $h'$  profiles where the densities were below  $1000 \text{ el cm}^{-3}$ , a limitation that means the technique is typically sensitive in the altitude range 50–60 km during SPEs. The calculated values of  $\beta$  and  $h'$  were then applied to the LWPC model to determine how they would effect radio propagation conditions compared with normal, quiet-time, conditions. They were only applied to the part of the propagation path poleward of the  $L = 4$  boundary which here overlaps with the low conductivity part of the path over the Antarctic ice cap. This experimental configuration is expected to be one of the most sensitive ways of monitoring polar precipitation events as the very low surface conductivities enhance the SPE effects [*Westerlund et al., 1969*].

[22] One test of the confidence in the radio propagation calculations is to consider the accuracy with which LWPC modeled the NPM–Halley quiet-time diurnal variation, as shown in Figure 5. During the daytime portion of the path i.e., that part of the day when all of the GCP is influenced by solar ionizing radiation (1600–0400 UT), both the absolute levels and variation with time are very well



described by LWPC. This was achieved by using the empirical daytime ionospheric model developed by *McRae and Thomson* [2000]. During the nighttime portion of the diurnal curve, i.e., 0400–1600 UT, the absolute values and variation with time are less well represented by LWPC, with discrepancies of typically –10 dB. Currently, the best nighttime model is provided by the LWPC ionosphere model [*Ferguson and Snyder*, 1990], although it is hoped that an improved parameterization can be developed in the near future.

[23] Comparing the change in amplitude of NPM at Halley during the SPE with the GOES satellite proton flux measurements we can observe a good correlation (Figure 8). Clearly, the variability observed in the VLF data is primarily caused by the proton fluxes, and thus SPE produced ionization dominates all other sources at these altitudes, e.g., relativistic electron precipitation events, and no other precipitation types need to be considered in this 4–5 November 2001 event. In earlier studies, authors have reported various SPE-produced signatures in VLF subionospheric propagation data, which has made using the data problematic. Our work strongly suggests that VLF subionospheric propagation is a reliable tool for the study of SPEs and that it is particularly effective when used in conjunction with an atmospheric model such as SIC.

[24] It was also possible to relate the GOES proton fluxes to the Wait parameters  $\beta$  and  $h'$ . It is thus possible to confidently predict the change in ionospheric reflection height as a function of proton fluxes in the >50 MeV range, although determining the relationship of fluxes to  $\beta$  is less well described at present and more work needs to be done on this in the future. Consequently, these results suggest that the assumption made during the SIC modeling runs of the 4–5 November 2001, SPE of only having proton precipitation and no significant energetic electron precipitation was reasonable. This in turn lends confidence to the reductions in ozone, and increases in odd nitrogen, at about 60 km predicted by the SIC model [*Verronen et al.*, 2002] during intense solar proton events.

[25] **Acknowledgments.** This work was supported in part by the LAPBIAT programme of the European Commission, project HRPI-CT-2001-00132.

[26] Arthur Richmond thanks Charles Jackman and Alexander Shirochkov for their assistance in evaluating this paper.

## References

- Banks, P. M., and G. Kockarts (1973), *Aeronomy*, vol. B, pp. 32–61, chap. 15, Elsevier, New York.
- Barr, R., D. L. Jones, and C. J. Rodger (2000), ELF and VLF radio waves, *J. Atmos. Sol. Terr. Phys.*, **62**, 1689–1718.
- Chabrilat, S., G. Kockarts, D. Fonteyn, and G. Brasseur (2002), Impact of molecular diffusion on the CO<sub>2</sub> distribution and the temperature in the mesosphere, *Geophys. Res. Lett.*, **29**(15), 1729, doi:10.1029/2002GL015309.
- Clilverd, M. A., C. J. Rodger, and N. R. Thomson (1999), Sunrise effects on VLF signals propagating over a long north-south path, *Radio Sci.*, **34**, 939–948.
- Clilverd, M. A., C. J. Rodger, N. R. Thomson, J. Lichtenberger, P. Steinbach, P. Cannon, and M. J. Angling (2001), Total solar eclipse effects on VLF signals: Observations and modelling, *Radio Sci.*, **36**, 773–788.
- Cummer, S. A., T. F. Bell, U. S. Inan, and D. L. Chenette (1997), VLF remote sensing of high-energy auroral particle precipitation, *J. Geophys. Res.*, **102**, 7477–7484.
- Dowden, R. L., C. D. D. Adams, J. B. Brundell, and P. E. Dowden (1994), Rapid onset, rapid decay (RORD), phase and amplitude perturbations of VLF subionospheric transmissions, *J. Atmos. Terr. Phys.*, **56**, 1513–1527.
- Ebel, A. (1980), Eddy diffusion models for the mesosphere and lower-thermosphere, *J. Atmos. Terr. Phys.*, **42**, 617–628.
- Ferguson, J. A., and F. P. Snyder (1990), Computer programs for assessment of long wavelength radio communications, *Tech. Doc. 1773*, Natl. Ocean Syst. Cent., Alexandria, Va.
- Hargreaves, J. K. (1992), *The Solar-Terrestrial Environment*, Cambridge Atmos. and Space Sci. Ser., Cambridge Univ. Press, New York.
- Hedin, A. E. (1991), Extension of the MSIS thermospheric model into the middle and lower atmosphere, *J. Geophys. Res.*, **96**, 1159–1172.
- Jackman, C. H., J. E. Nielson, D. J. Allen, M. C. Cerniglia, R. D. McPeters, A. R. Douglass, and R. B. Rood (1993), The effects of the October 1989 solar proton events on the stratosphere as computed using a 3-dimensional model, *Geophys. Res. Lett.*, **20**, 459–462.
- McRae, W. M., and N. R. Thomson (2000), VLF phase and amplitude: daytime ionospheric parameters, *J. Atmos. Sol. Terr. Phys.*, **62**, 609–618.
- Murtagh, D., et al. (2002), An overview of the Odin atmospheric mission, *Can. J. Phys.*, **80**, 309–319.
- Potemra, T. A., A. J. Zmuda, C. R. Haave, and B. W. Shaw (1967), VLF phase perturbations produced by solar protons in the event of February 5, 1965, *J. Geophys. Res.*, **72**, 6077–6089.
- Reagan, J. B., and T. M. Watt (1976), Simultaneous satellite and radar studies of the D-region ionosphere during the intense solar particle events of August 1972, *J. Geophys. Res.*, **81**, 4579–4589.
- Reeves, G. D., T. E. Cayton, S. P. Gary, and R. D. Belan (1992), The great solar energetic particle events of 1989 observed from geosynchronous orbit, *J. Geophys. Res.*, **97**, 6219–6226.
- Reid, G. C., S. Solomon, and R. R. Garcia (1991), Response of the middle atmosphere to solar proton events of August–December, 1989, *Geophys. Res. Lett.*, **18**, 1019–1022.
- Rishbeth, H., and O. K. Garriott (1969), *Introduction to Ionospheric Physics*, Elsevier, New York.
- Rusch, D. W., J.-C. Gerard, S. Solomon, P. J. Crutzen, and G. C. Reid (1981), The effect of particle precipitation events on the neutral and ion chemistry of the middle atmosphere – 1. Odd nitrogen, *Planet. Space Sci.*, **29**, 767–774.
- Shea, M. A., and D. F. Smart (1990), A summary of major solar proton events, *Sol. Phys.*, **127**, 297–320.
- Shirochkov, A., L. N. Makarova, S. N. Sokolov, and W. R. Sheldon (2004), Ionospheric effects of the simultaneous occurrence of a solar proton event and relativistic electron precipitation as recorded by ground-based instruments at different latitudes, *J. Atmos. Sol. Terr. Phys.*, **66**, 1035–1045.
- Solomon, S., G. C. Reid, D. W. Rusch, and R. J. Thomas (1983), Mesospheric ozone depletion during the solar proton event of July 13, 1982: 2. Comparisons between theory and measurements, *Geophys. Res. Lett.*, **10**, 257–260.
- Thomas, L., and M. R. Bowman (1986), A study of pre-sunrise changes in negative ions and electrons in the D-region, *Ann. Geophys.*, **4**, 219–228.
- Tobiska, W. K., T. Woods, F. Eparvier, R. Viereck, L. D. B. Floyd, G. Rotman, and O. R. White (2000), The SOLAR2000 empirical solar irradiance model and forecast tool, *J. Atmos. Sol. Terr. Phys.*, **62**, 1233–1250.
- Turunen, E., H. Matveinen, J. Tolvanen, and H. Ranta (1996), D-region ion chemistry model, in *STEP Handbook of Ionospheric Models*, edited by R. W. Schunk, pp. 1–25, SCOSTEP Secretariat, Boulder, Colo.
- Verronen, P. T., E. Turunen, T. Ulich, and E. Kyrölä (2002), Modelling the effects of the October 1989 solar proton event on mesospheric odd nitrogen using a detailed ion and neutral chemistry model, *Ann. Geophys.*, **20**, 1967–1976.
- Wait, J. R., and K. P. Spies (1964), Characteristics of the Earth-ionosphere waveguide for VLF radio waves, *Tech. Note 300*, Natl. Bur. of Stat., Boulder, Colo.
- Westerlund, S., F. H. Reeder, and C. Abom (1969), Effects of polar cap absorption events on VLF transmissions, *Planet. Space Sci.*, **17**, 1329–1374.
- A. Botman and M. A. Clilverd, Physical Sciences Division, British Antarctic Survey, Madingley Road, Cambridge, CB3 0ET, UK. (aurelien.botman@cantab.net; m.clilverd@bas.ac.uk)
- C. J. Rodger and N. R. Thomson, Department of Physics, University of Otago, Dunedin, New Zealand. (crodrger@physics.otago.ac.nz; thomson@physics.otago.ac.nz)
- A. Seppälä, Finnish Meteorological Institute, P.O. Box 503 (Vuorikatu 15 A), FI-00101 Helsinki, Finland. (annika.seppala@fmi.fi)
- E. Turunen and T. Ulich, Sodankylä Geophysical Observatory, FIN-99600 Sodankylä, Finland. (esa@sgo.fi; thu@sgo.fi)